Journal of the Korean Society for Nondestructive Testing
Vol. 28, No. 6 (2008. 12)

On the Beam Focusing Behavior of Time Reversed Ultrasonic Arrays Using a Multi-Gaussian Beam Model

Hyunjo Jeong*†, Jeong-Sik Lee*, Yon-Ho Jeong* and Sung-Min Bae*

Abstract One of the fundamental features of time reversal acoustic (TRA) techniques is the ability to focus the propagating ultrasonic beam to a specific point within the test material. Therefore, it is important to understand the focusing properties of a TR device in many applications including nondestructive testing. In this paper, we employ an analytical scheme for the analysis of TR beam focusing in a homogeneous medium. More specifically, a nonparaxial multi-Gaussian beam (NMGB) model is used to simulate the focusing behavior of array transducers composed of multiple rectangular elements. The NMGB model is found to generate accurate beam fields beyond the nonparaxial region. Two different simulation cases are considered here for the focal points specified on and off from the central axis of the array transducer. The simulation results show that the focal spot size increases with increasing focal length and focal angle. Furthermore, the maximum velocity amplitude does not always coincide with the specified focal point. Simulation results for the off-axis focusing cases do demonstrate the accurate steering capability of the TR focusing.

Keywords: Time Reversal Focusing, Multi-Gaussian Beam, Array Transducers, Focusing Properties

1. Introduction

The ability of array transducers of multiple elements to steer, focus and scan interrogating beams inside test materials provides benefits over conventional ultrasonic technology. Beam steering to test objects with multiple angles from a single probe can greatly simplify the inspection of components with complex geometries, thus can greatly increase the probability of detection of anomalies. The ability to narrowly focus the beam provides enhanced spatial resolution for flaw detection and sizing. Focusing can also significantly improve signal-to-noise ratio in challenging applications. Ultrasonic phased array transducers are widely used in the area of nondestructive evaluation (NDE) and in many medical applications. Some of the attractive features of phased arrays include electronic focusing and steering capabilities. To generate a focused beam at any specified angle and distance, time delays are calculated and applied electronically to each element. However, these techniques suffer important limitations. They are all based on a priori knowledge of geometry and acoustic properties of the sample and assume that the sound velocity is known and constant in each medium.

Because of these limitations and in order to improve the flexibility of the focusing process, self-focusing techniques have been proposed. Time reversal acoustics (TRA) is one of the most interesting topics in this respect (Fink, 1992; Kim et al., 2006). One of the fundamental features of time reversal (TR) techniques is the ability to focus the propagating ultrasonic beam

Received: November 21, 2008, Revised: December 10, 2008, Accepted: December 13, 2008. * Division of Mechanical and Automotive Engineering, Wonkwang University, 344-2 Sinyong-Dong, Iksan, Jeonbuk 570-749, Korea, † Corresponding Author: hjjeong@wonkwang.ac.kr

to a specific point within the test material. In the first step of TR, each element of the array transducer transmits a wave and the propagating wave is recorded at a specified focal point. In the second step of TR, the recorded signals are time reversed and reemitted simultaneously by each element. After TR, the signals radiated by different elements arrive synchronously in phase (Choi et al., 2008). Thus, they are enhanced by each other and refocused. Compared to ultrasonic phased arrays, the TR focusing does not require a prior knowledge about the properties and structures of the media and the transducer. For further applications of TR technology in many testing situations, it is necessary to understand the TR process and focusing properties of array transducers.

In this paper, we employ an analytical scheme for the analysis of TR beam propagation and focusing in a homogeneous medium. More specifically, a nonparaxial multi-Gaussian beam (MGB) model is used to simulate the focusing behavior of the ultrasonic beam emitted from an array transducer composed of multiple rectangular elements. The use of nonparaxial MGB model is validated first. The simulation results on focusing behavior as a function of focal length and focal angle are then presented.

2. Multi-Gaussian Beam Models for a Contact Transducer

The radiation beam fields from an array transducer of multiple elements can be calculated by simply superposing individual pressure field from each element. A Rayleigh–Sommerfeld integral model provides exact solutions for a piston transducer in the fluid case. For a contact transducer radiating into a solid, a similar Rayleigh–Sommerfeld integral type of model can also be derived(Schmerr, 1998). The velocity field of predominant compressional (P-) wave in the solid is given by

$$\mathbf{v}(\mathbf{x},\omega)=\frac{-i\omega\,\mathbf{d}_{p1}}{2\pi\rho_1 c_{p1}^2}\int_{S_T} p_0\,K_p(\theta')\frac{\exp(ik_{p1}r)}{r}\,dS_T \quad (1)$$

Where ω is the circular frequency, ρ_1 the density of the solid, c_{p1} the P-wave speed, P_0 the pressure over the transducer surface, and $\mathbf{d}_{p1}$ the polarization vector and the wave number of the P-wave. Here $r=|\mathbf{x}-\mathbf{x}_0|$ is the distance from an arbitrary point $\mathbf{x}_0(x_0,\ y_0,\ z_0\ =\ 0)$ on the transducer surface to an observation point $\mathbf{x}(x,\ y,\ z)$, in the solid. S_T is the area of the transducer. Unlike the immersion transducer case, an angular dependent directivity function $K_p(\theta')$ is present for the solid case, given by the expression

$$K_p(\theta')=\frac{\cos\theta'\kappa_1^2(\kappa_1^2/2-\sin^2\theta')}{2G(\sin\theta')} \quad (2)$$

where $G(x)=(x^2-\kappa_1^2/2)^2+x^2\sqrt{1-x^2}\sqrt{\kappa_1^2-x^2}$, $\kappa_1=c_{p1}/c_{s1}$, and θ' is the angle between the $\mathbf{r}$ vector and the normal to the transducer surface. Here, c_{s1} is the shear wave speed.

Although eqn. (1) can be served to exactly calculate the radiation beam field into solids, it is computationally inefficient. A multi-Gaussian beam model, based on a paraxial approximation, can be a practical, efficient transducer modeling tool for many NDE applications. Schmerr and Song(2007) give a complete description of Gaussian beam theory and its use for modeling sound beams generated by ultrasonic transducers in the form of a multi-Gaussian beam model. Since a multi-Gaussian transducer beam model is an approximate paraxial solution, there will be some situations where a paraxial multi-Gaussian beam model will lose accuracy. More recently, Zhao and Gang(2008) proposed a more accurate solution to eliminate limitations of paraxial approximation. Based on a nonparaxial approximation for the radiation distance r, they derived the following nonparaxial multi-Gaussian beam (NMGB) model for eqn. (1) for a planar rectangular transducer with sides of lengths ($2a_1$,

$2a_2$) in the (x, y) directions:

$$\mathbf{v}(\mathbf{x},\omega) = \frac{-i\omega K_p(\theta)\,\mathbf{d}_{p1}}{2\pi\rho_1 c_{p1}^2}\exp(ik_{p1}R)\sum_{m=1}^{10}\sum_{n=1}^{10}\frac{A_m A_n}{\sqrt{1+iB_m R/D_1}\sqrt{1+iB_n R/D_2}} \times\exp\left[-ik_{p1}\left(\frac{1}{2}\mathbf{X}^T\left[\mathbf{M}_1^p(R)\right]_{mn}\mathbf{X}\right)\right] \quad (3)$$

where $\mathbf{X}^T=(x,y)$, A_m, B_m, A_n, B_n are complex coefficients of Wen and Breazeale(1988), $D_1=k_{p1}a_1^2/2$, $D_2=k_{p1}a_2^2/2$, $R=\sqrt{x^2+y^2+z^2}$, and

$$\left[\mathbf{M}_1^p(R)\right]_{mn}=\begin{bmatrix}\dfrac{1/R}{1+iB_mR/D_1} & 0\\ 0 & \dfrac{1/R}{1+iB_nR/D_2}\end{bmatrix}.$$

In eqn. (3) θ is the angle between the **R** vector and the normal to the transducer surface. When compared with the exact Rayleigh-Sommerfeld integral model, the NMGB model of eqn. (3) was found to give almost the same results in both paraxial and nonparaxial regions. Because of the good accuracy of the NMGB model, it will be employed in calculating TR beam fields in the next section.

3. Simulations of TR Beam Focusing

The time reversal process for a beam focusing is composed of two steps. In the first step of TR, each element of the array transducer transmits a wave and the propagating wave is recorded individually at a specified focal point. In the second step of TR, the recorded signals are time reversed and reemitted simultaneously by each element. After TR, the signals radiated by different elements arrive synchronously in phase. Thus, they are enhanced by each other and refocused. The nonparaxial MGB model, eqn. (3), will be employed for calculating all the beam fields in the TR process.

Fig. 1 shows the schematic illustration of an array transducer composed of multiple rectangular elements. The array transducer used for simulations is a 32 element linear array with center frequency 5 MHz. The size of rectangular element is 0.8×10 mm in the x- and y-directions, and the inter-element gap is 0.2 mm. The x- and z-axes are defined along the array direction of the transducer and normal to the transducer, respectively, and the origin is located at the center of the array transducer. Two different simulations are considered here. In the first simulation, the focal points are placed on the central axis of the transducer by setting $\theta=\phi=0^\circ$, and four different focal distances are used: F=25, 50, and 100 mm. In the second simulation, the focal points with four different steering angles: $\theta_s=0^\circ,5^\circ,30^\circ,45^\circ$ are used with fixed focal distance of 80 mm and $\phi=0^\circ$. The propagating medium is steel, characterized by the sound speed c_{p1}=5900 m/s, c_{s1}=3200 m/s, and ρ_1=7900 kg/m^3.

The velocity field for each element will be calculated in the frequency domain, therefore it will be given by a complex value. Time reversal is the same as phase conjugation. The time reversal operation at the focal point is then performed by taking the complex conjugate of the received velocity. This quantity of complex conjugate will be referred to as "TR coefficient" here. The TR coefficient is then multiplied as an input parameter when the beam is reradiated all together from the N elements at the initial transducer position. The total beam fields after the TR process can be obtained by simple

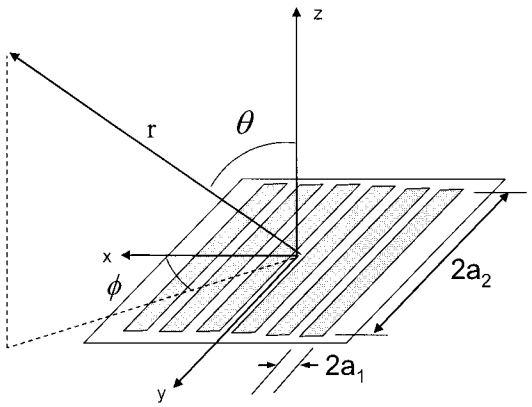

Fig. 1 Schematic illustration of an array transducer with rectangular elements

superposition of individual field. For a linear phased array transducer with N elements, the P-wave velocity field is then calculated by

$$\mathbf{v}_{total}(\mathbf{x},\omega)=\sum_{n=1}^{N}V_n^*(F,\theta_s)\mathbf{v}_n(\mathbf{x},\omega) \tag{4}$$

where $V_n^*(F,\theta_s)$ is the TR coefficient, and ( )* denotes the complex conjugate.

4. Results and Discussion

As mentioned previously, the current TR process can be shown to be equivalent to applying the necessary time delay to each element of the phased array transducer of the same structure to focus its beam at the desired focal point. The TR coefficient for each element, $V_n^*(F,\theta_s)$, is obtained as a complex number, so its phase angle can be calculated and unwrapped. From this phase angle, the time delay for the nth element is given by

$$\Delta t_n=\frac{\Delta\varphi_n}{\omega} \tag{5}$$

Fig. 2 shows the time delays obtained from eqn. (5) when $\theta=30^\circ$ and F=80 mm. In fact, they are exactly the same as those calculated from the focal law of phased array transducers (Krautkramer, 1990).

Fig. 3 shows the simulation results when the focal length varies along the central axis of the array transducer (on-axis focusing). The figures at the top line represent the 2D velocity pattern in the x-z plane, while those figures at the middle and bottom lines respectively show the velocity distribution along the central z axis and along the horizontal axis passing through the maximum amplitude of velocity profile. Figs. 3(a1)-(a3), (b1)-(b3), (c1)-(c3), and (d1)-(d3) show simulated velocity distributions with specified focal distances of ∞, 25, 50, and 100 mm, respectively.

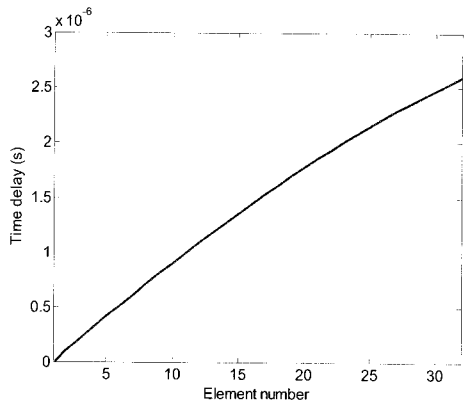

Fig. 2 Calculated time delays by using the TR coefficient for θ=30° and F=80 mm

When all the 32 elements are radiated simultaneously without time reversal focusing process, the results are shown in Fig. 3(a1)-(a3). In this case, the transition range of an array transducer is defined, in a similar manner to a single transducer, as (Krautkramer, 1990; Azar et al., 2000)

$$z_{TR}=\frac{D^2}{4\lambda} \tag{6}$$

where D is the overall dimension of the array transducer, and λ is the wavelength. This transition range separates the near field from the far field of the array. It is known that focusing of array transducers may increase the system resolution for imaging targets that are located within the near field of the array aperture, that is, at distances less than z_{TR}. For the current setup of the array transducer, z_{TR} is calculated as 214.25 mm, and the simulation, Fig. 3(a2), accurately predicts this value.

The spatial focusing property of the TR array is important in various applications including nondestructive testing, so we need to examine the resolution limit of the TR focused signal. In a homogeneous medium it is known that the time-reversed and backpropagated signal due to a point source will focus in a region around the original focal point with spatial width (or the focal spot size) of order (Tsogka and Papanicolaou, 2002)

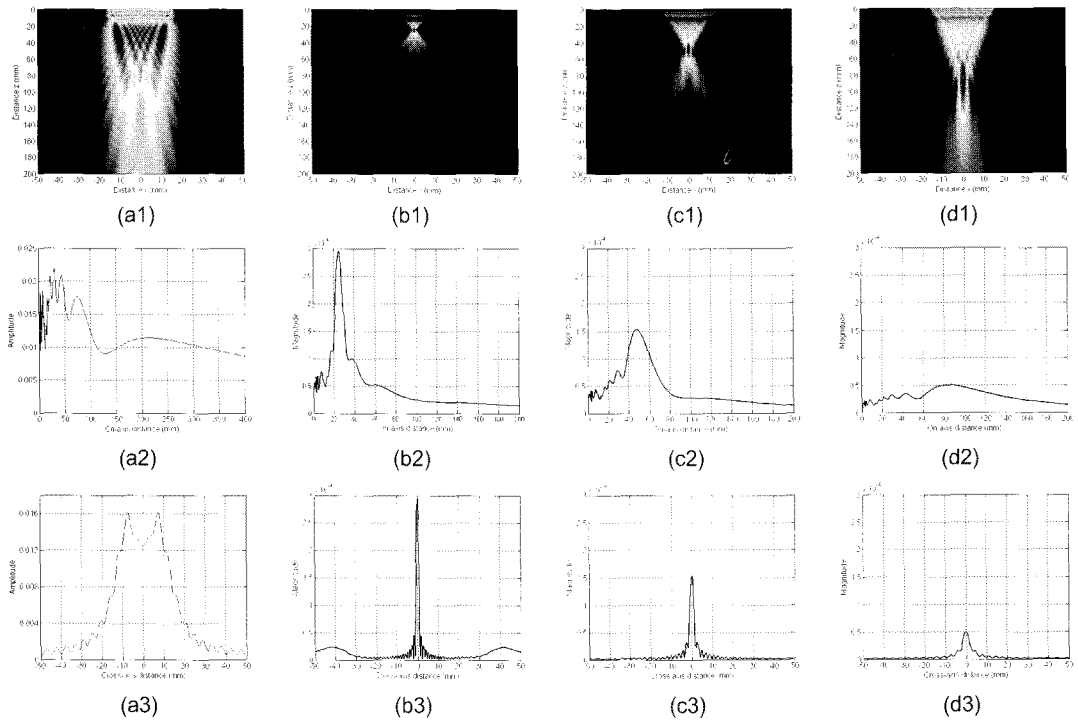

Fig. 3 Simulation results for time reversal focusing with different focal positions located along the central axis of the array transducer: (a) Unfocused (F=∞), (b) F=25 mm, (c) F=50 mm, (d) F=100 mm

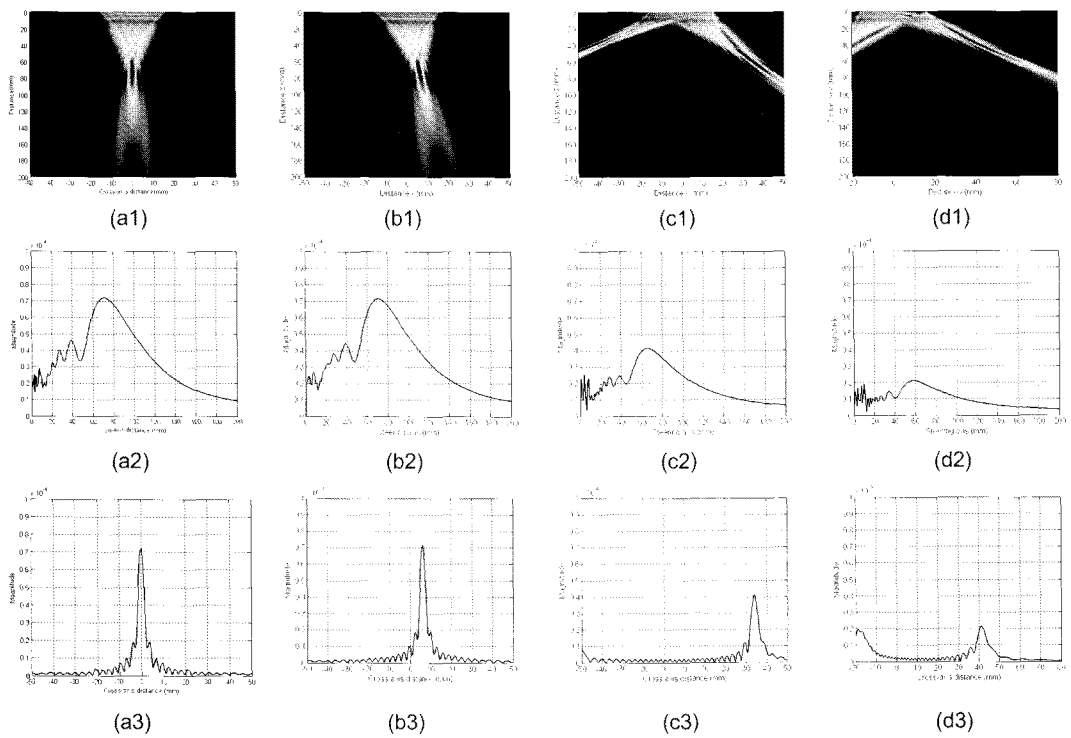

Fig. 4 Simulation results for time reversal focusing when the focal points are initially specified at: (a) $\theta = 0°, \mathrm{F} = 80\,\mathrm{mm}$, (b) $\theta = 5°, \mathrm{F} = 80\,\mathrm{mm}$, (c) $\theta = 30°, \mathrm{F} = 80\,\mathrm{mm}$, (d) $\theta = 45°, \mathrm{F} = 80\,\mathrm{mm}$

$$d = \frac{\lambda L}{D} \tag{7}$$

where λ and D were defined previously, and L is the distance between the array sensor and the focal point. Eqn. (7) tells that the focal size increases with increasing focal depth for fixed λ and D. Increased focal spot size also means decrease of peak velocity, and this is clearly noticed in the simulation results of Fig. 3. For current setup, λ=1.18 mm and D=31.8 mm. The estimated focal size by eqn. (7) for the simulation case of Fig. 3(c3) is 1.76 mm when the actual focal length of F_{act}= 47.4 mm is used. In this case, the measured spot sizes at -3 dB and -6 dB from Fig. 3(c3) are about 1.7 mm and 2.35 mm, respectively.

Fig. 4 shows the simulation results when the focal points are initially specified at certain angles θ from the central axis with the focal lengths fixed at 80 mm (off-axis focusing). Figures 4(a)-(d) represent the simulation results for θ=0°,5°,30°, and 45°, respectively. First of all, we notice the steered, focused beam patterns. The actual steering angles measured from the 2D velocity patterns, Figs. 4(a1)-(d1), agree with the originally specified angles within ±0.5°. These results indicate the steering capability of the TR focusing technique. It is also observed that the focal spot size increases as the off-axis focusing angle increases. Because of this, the maximum velocity also decreases with increasing focusing angle.

Figs. 3 and 4 also demonstrate another important factor that the maximum pressure does not always occur at the original focal point. Fig. 4 shows that the maximum pressure occurs at approximately 82 mm when the focal point is set at 100 mm. This is due to the diffraction effect that tends to bring the point of maximum beam intensity in the steering direction nearer to the transducer(Krautkramer, 1990). The deviation of the actual focal point from the original focal depth also increases with increasing focal distance.

5. Conclusions

A nonparaxial multi-Gaussian beam model (NMGB) was employed to examine the spatial focusing properties of array transducer beam when the time reversal focusing technique was applied in a single propagating medium. The NMGB model was found to generate accurate beam fields both within and beyond the nonparaxial regions. Therefore, it may be utilized as an efficient computational tool for simulating radiation beam fields of array transducers. The simulated 2-D beam patterns, and velocity distributions along the steered directions and along the cross-axes passing through the maximum amplitude points were analyzed. The current TR process is actually equivalent to applying the necessary time delay to each element of the phased array transducer of the same structure to focus its beam at the desired focal point. Therefore, the general behavior of TR beam focusing was pretty similar to the focusing properties of linear phased array transducers(Song et al., 2000). Another important factor to be noticed is the accurate steering capability of the TR focusing. The TR method, however, would provide better overall focusing and steering in real testing situations because the actual field propagated within the sample is used for the beam focusing. Future work should address this issue through experimental verification.

Acknowledgement

This work was supported by 2008 Nuclear R&D program through the Korea Science and Engineering Foundation funded by the Ministry of Education, Science and Technology

References

Azar, L., Shi, Y. and Wooh, S. C. (2000) Beam Focusing Behavior of Linear Phased Arrays,

NDT&E International, Vol. 33, pp. 189–198

Choi, B. K., Kim, B.-C., Sutin, A. and Sarvazyan, A. (2008) Ultrasonic Focused Waveform Generation Using Time Reversal Acoustic Focusing System, *Journal of Mechanical Science and Technology*, Vol. 22, pp. 699~707

Fink, M. (1992) Time Reversal of Ultrasonic Fields. I. Basic Principles, *IEEE Trans. Ultrason. Ferroelectr. Freq. Control*, Vol. 39, pp. 555-566

Kim, H.-J., Song, S.-J., Thompson, R. B. and Kim, J.-H. (2006) Use of Time Reversal Techniques for Focusing of Ultrasonic Array Transducer Beams, *Journal of the Korean Society for Nondestructive Testing*, Vol. 26, pp. 190-197

Krautkramer, J. and Krautkramer, H. (1990) *Ultrasonic Testing of Materials*, 4th Eds., Springer- Verlag, New York, NY

Schmerr, L. W. (1998) Fundamentals of Ultrasonic Nondestructive Evaluation – A Modeling Approach, Plenum Press, New York, NY

Schmerr, L. W. and Song, S.-J. (2007) Ultrasonic Nondestructive Evaluation Systems: Models and Measurements, Springer, New York, NY

Song, S.-J., Shin, H. J. and Jang, Y. H. (2000) Calculations of Radiation Field of Phased Array Transducers Using Boundary Diffraction Wave Model, *in Proc. 15th WCNDT*, Rome, Italy, Oct. 15-20

Tsogka, C. T. and Papanicolaou, G. (2002) Time Reversal through a Solid-Liquid Interface and Super-Resolution, *Inverse Problems*, Vol. 18, pp. 1639-1657

Wen, J. J. and Breazeale, M. A. (1988) A Diffraction Beam Field Expressed as the Superposition of Gaussian Beams, *Journal of the Acoustical Society of America*, Vol. 83, pp. 1752 –1756

Zhao X. and Gang, T. (2008) Nonparaxial Multi-Gaussian Beam Models and Measurement Models for Phased Array Transducers, Articles in Press, *Ultrasonics*